Trans. Japan Soc. Aero. Space Sci.
Vol. 55, No. 4, pp. 237–243, 2012

Electric Current Analysis for Thick Laminated CFRP Composites*

By Akira TODOROKI

Tokyo Institute of Technology, Tokyo, Japan

(Received November 11th, 2011)

This paper deals with a new lamination theory to calculate the electric current density on carbon fiber reinforced plastic (CFRP) laminates. Unidirectional CFRP has strong orthotropic electric conductance. When electric current is applied to the surface of a CFRP plate, the electric voltage field is not uniform in the thickness direction for thick CFRP. The electric current concentrates near the surface where the electric current is applied to thick CFRP laminates. In this study, a new lamination theory for thick CFRP laminates is proposed. The theory for thick CFRP assumes a non-uniform electric voltage distribution in the thickness direction. For non-thick and non-thin CFRP plates, an approximation method is proposed. To obtain the shape of the non-uniform voltage distribution, the analytical results of thick unidirectional ply from a previous paper is adopted as a contribution function to calculate the effective conductance of the thick CFRP laminate. Cross-sectional two-dimensional (2D) FEM analysis is used to obtain the contribution function for the non-thick CFRP plate. The proposed methods are applied to two cases of the thick CFRP plates, and the results are compared with the three-dimensional (3D) FEM results. Consequently, the new lamination theory is shown to be very effective for the CFRP plates.

Key Words: Composite Materials, Potential Flow, Analysis, Electric Current, Orthotropic Electric Conductivity

1. Introduction

Carbon-fiber-reinforced polymer (CFRP) composites have highly electrically conductive carbon fibers. The matrix resin, however, is usually an electrical insulator. This makes it a material with significantly strong anisotropic electric conductance.[1] Although electric conductance in the fiber direction is very high, the electric conductance in the transverse or thickness direction consists of a carbon fiber contact network, which has extremely low conductance in the two orthogonal directions compared with the fiber direction.[2]

When a lightning strike occurs to the anisotropic electrically conductive thick CFRP composites, electric current flow becomes very complicated compared with the very thin CFRP, because the thin CFRP, the electric voltage is uniform in the thickness direction and there is no electric current in this direction. The electric current for the thin CFRP can be calculated using two-dimensional (2D) analysis because it has no electric current in the thickness direction. However, for the thick CFRP, it is quite difficult to obtain an appropriate electric current distribution using 2D analysis because of the existence of an electric voltage distribution in the thickness direction. This makes it very difficult to determine the leakage electric current in the anti-lightning copper mesh in aircraft wings. In the previous paper,[3] an analytical method using the potential flow of a perfect fluid was performed for the thick unidirectional CFRP. An analytical method was then applied to the thick cross-ply laminate to obtain approximate results. The method cannot be applied to general CFRP laminates that have angled plies. For the analysis of the electric current from a lightning strike, it is preferable to compute the electric current using 2D analysis instead of three-dimensional (3D) laminated structural analysis. The lamination theory for the electric conductance of a CFRP laminate, however, has not yet been published, except for a thin CFRP laminate.[4]

In this study, the lamination theory of electric conductance for a thin CFRP laminate is described first. A new lamination theory for a thick CFRP is then proposed to compute the electric current density using 2D-FEM analysis. The theory is applied to a typical thickness CFRP and the results are compared with 3D-FEM analysis.

2. Theory of CFRP Laminates of Electric Current

2.1. Theory of thin CFRP laminates

For unidirectional CFRP, all fibers are aligned in an identical direction, and this causes orthotropic electrical conductance. Electric current in the orthotropic materials can be obtained in a similar manner to thermal conductance for the orthotropic materials.[5] Let us assume that the fiber direction for the unidirectional CFRP is along the x-axis; the transverse direction is then the y-axis and the thickness direction is the z-axis. Using the electric voltage potential function ϕ, the electric current densities i_x, i_y, i_z are obtained as follows.

$$i_x = -\sigma_x \frac{\partial \phi}{\partial x}, \quad i_y = -\sigma_y \frac{\partial \phi}{\partial y}, \quad i_z = -\sigma_z \frac{\partial \phi}{\partial z}, \qquad (1)$$

where σ_x, σ_y, σ_z are electric conductance for unidirectional CFRP in the fiber, transverse and thickness directions, respectively.

*Translated from Journal of the Japan Society for Aeronautical and Space Sciences, Vol. 59, No. 692, 2011, pp. 252–257

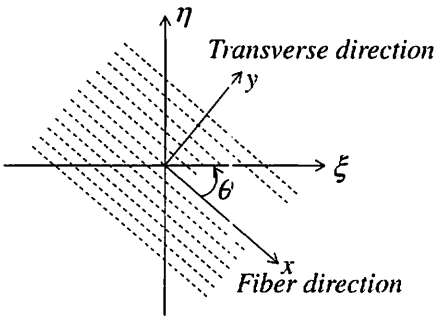

Fig. 1. Rotated coordinate.

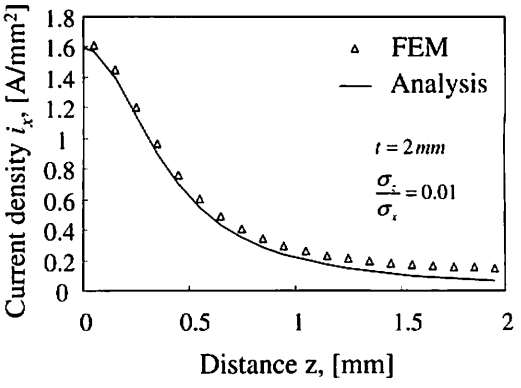

Fig. 2. Distribution of electric current density for unidirectional CFRP.[3)]

Initially, we consider whether the CFRP plate is thin enough. If the plate is thin enough, the electric current does not flow in the thickness direction: this implies the electric voltage is uniform in the thickness direction. Xiao et al.[4)] presented a lamination theory of electric conductance in the theory of piezoresistivity of a CFRP laminate. Since there is no electric current in the thickness direction, Eq. (1) reduces to:

$$i_x = -\sigma_x \frac{\partial \phi}{\partial x}, \quad i_y = -\sigma_y \frac{\partial \phi}{\partial y}. \tag{2}$$

We now consider the case of off-axis flow where the flow direction is different from the fiber direction. A rotated rectangular coordinate ξ–η is defined as shown in Fig. 1: the ξ–η coordinate is made by rotating the x–y coordinate through an angle θ.

The electric current density in the ξ-direction (i_ξ) and electric current density in the η-direction (i_η) are defined as follows.[4)]

$$\begin{pmatrix} i_\xi \\ i_\eta \end{pmatrix} = \begin{pmatrix} \sigma_x \cos\theta & \sigma_y \sin\theta \\ -\sigma_x \sin\theta & \sigma_y \cos\theta \end{pmatrix} \begin{pmatrix} \dfrac{\partial \phi}{\partial x} \\ \dfrac{\partial \phi}{\partial y} \end{pmatrix}. \tag{3}$$

The electric voltage potential difference of the x–y coordinate is transformed to the ξ–η coordinate as follows.

$$\begin{pmatrix} \dfrac{\partial \phi}{\partial \xi} \\ \dfrac{\partial \phi}{\partial \eta} \end{pmatrix} = \begin{pmatrix} \cos\theta & \sin\theta \\ -\sin\theta & \cos\theta \end{pmatrix} \begin{pmatrix} \dfrac{\partial \phi}{\partial x} \\ \dfrac{\partial \phi}{\partial y} \end{pmatrix}. \tag{4}$$

Substituting Eq. (4) into Eq. (3) gives

$$\begin{pmatrix} i_\xi \\ i_\eta \end{pmatrix} = \begin{pmatrix} \sigma_{\xi\xi} & \sigma_{\xi\eta} \\ \sigma_{\eta\xi} & \sigma_{\eta\eta} \end{pmatrix} \begin{pmatrix} \dfrac{\partial \phi}{\partial \xi} \\ \dfrac{\partial \phi}{\partial \eta} \end{pmatrix}, \tag{5}$$

where

$$\begin{aligned} \sigma_{\xi\xi} &= \sigma_x \cos^2\theta + \sigma_y \sin^2\theta \\ \sigma_{\xi\eta} &= \sigma_{\eta\xi} = -(\sigma_x - \sigma_y)\sin\theta\cos\theta \\ \sigma_{\eta\eta} &= \sigma_y \cos^2\theta + \sigma_x \sin^2\theta. \end{aligned} \tag{6}$$

A laminated CFRP is made by stacking thin plies at various angles. For a thin CFRP laminate, electric voltage is uniform in the thickness direction in all the plies. The average electric current density can easily be obtained by the integration of each electric current density as follows.

$$\begin{aligned} i_\xi &= \frac{1}{t}\int_0^t \left(\sigma_{\xi\xi}\frac{\partial \phi}{\partial \xi} + \sigma_{\xi\eta}\frac{\partial \phi}{\partial \eta}\right) dz \\ i_\eta &= \frac{1}{t}\int_0^t \left(\sigma_{\eta\xi}\frac{\partial \phi}{\partial \xi} + \sigma_{\eta\eta}\frac{\partial \phi}{\partial \eta}\right) dz, \end{aligned} \tag{7}$$

$$\begin{pmatrix} i_\xi \\ i_\eta \end{pmatrix} = \begin{pmatrix} \frac{1}{t}\int_0^t \sigma_{\xi\xi}\,dz & \frac{1}{t}\int_0^t \sigma_{\xi\eta}\,dz \\ \frac{1}{t}\int_0^t \sigma_{\eta\xi}\,dz & \frac{1}{t}\int_0^t \sigma_{\eta\eta}\,dz \end{pmatrix} \begin{pmatrix} \dfrac{\partial \phi}{\partial \xi} \\ \dfrac{\partial \phi}{\partial \eta} \end{pmatrix}, \tag{8}$$

$$\begin{pmatrix} i_\xi \\ i_\eta \end{pmatrix} = \begin{pmatrix} C_{\xi\xi} & C_{\xi\eta} \\ C_{\eta\xi} & C_{\eta\eta} \end{pmatrix} \begin{pmatrix} \dfrac{\partial \phi}{\partial \xi} \\ \dfrac{\partial \phi}{\partial \eta} \end{pmatrix}, \tag{9}$$

where t is the thickness of the thin CFRP laminate. When the thin laminate consists of N plies of equal thickness t_p, C_{mn} ($m, n = \xi, \eta$) is obtained as follows.

$$\begin{aligned} C_{\xi\xi} &= \frac{1}{t}\int_0^t \sigma_{\xi\xi}\,dz = \sum_{k=1}^{N} \frac{t_p}{t}\sigma_{\xi\xi}^k, \\ C_{\xi\eta} = C_{\eta\xi} &= \frac{1}{t}\int_0^t \sigma_{\xi\eta}\,dz = \sum_{k=1}^{N} \frac{t_p}{t}\sigma_{\xi\eta}^k, \\ C_{\eta\eta} &= \frac{1}{t}\int_0^t \sigma_{\eta\eta}\,dz = \sum_{k=1}^{N} \frac{t_p}{t}\sigma_{\eta\eta}^k, \end{aligned} \tag{10}$$

where N is the total number of plies, and σ^k is the electric conductance calculated using Eq. (6) for the kth ply.

From Eqs. (6) and (10), we observe that the interaction term $C_{\xi\eta}$ becomes zero when the number of angle plies of the target CFRP laminate is balanced (i.e. when the total sum of the angles of the angle plies is zero).

2.2. Thick laminated CFRP

As described in the previous paper,[3)] the thin CFRP plate theory cannot be applied to the thick CFRP components. For the thick unidirectional CFRP case, the exact difference in the voltages can be obtained when the electric current density i_x is divided by electric conductance ($-\sigma_x$). Figure 2 shows the electric current density of the unidirectional

CFRP: the thickness is 2 mm and the spacing between the electrodes is 8 mm. The distribution of the difference in the voltages in the thickness direction is identical to this curve. The difference in the voltages is not uniform in the thickness direction for actual aircraft components made from CFRP laminates.

For a thin CFRP plate, every ply fully contributes as a path of electric current because the difference in the voltages is uniform throughout the thickness. For a thick CFRP plate in practice, however, the difference in the voltages decreases with the increase in the distance from the charged surface. This means the plies located far from the charged surface make small contributions to the path of the electric current in the thick CFRP plate used in practice. This indicates that the thin plate theory cannot be applied to the thick CFRP in practice. The distribution of the difference in the voltages throughout the thickness comes from the extremely small electric conductance in the thickness direction.

Thus, in this study, decreasing the difference in the voltages with increasing distance from the charged surface is replaced by a decrease in the cross-sectional area of the plies that are located far from the surface. This decrease in the cross-section of the current path is expressed using the contribution function F.

After the contribution function F is obtained, the modified lamination theory of electric conductance can be formulated. For a thin plate theory, the contribution function F is equal to one through the entire thickness. In practice, in a thick CFRP plate, F decreases with the increase in the distance from the charged surface. This means the cross-sectional area of the ply decreases. Since the contribution value at the surface where the electric current is applied is exactly equal to one, the contribution function can be obtained from the difference in the voltages by normalization with the surface value of the difference in the voltages. Figure 3 shows the contribution function of unidirectional CFRP.

Using the contribution function $F(\alpha)$ (where $\alpha = z/t$: the surface where the electrodes are located is set to $z = 0$), the values of Eq. (10) can be calculated as follows:

$$C_{\xi\xi} = \int_0^1 F(\alpha)\sigma_{\xi\xi}\,d\alpha = \sum_{k=1}^{N} \frac{t_p}{t} F_k \sigma_{\xi\xi}^k,$$

$$C_{\xi\eta} = \int_0^1 F(\alpha)\sigma_{\xi\eta}\,d\alpha = \sum_{k=1}^{N} \frac{t_p}{t} F_k \sigma_{\xi\eta}^k, \qquad (11)$$

$$C_{\eta\eta} = \int_0^1 F(\alpha)\sigma_{\eta\eta}\,d\alpha = \sum_{k=1}^{N} \frac{t_p}{t} F_k \sigma_{\eta\eta}^k,$$

where F_k is the value of $F(\alpha)$ at the middle of the kth ply. This multiplication of F_k is equal to a change of the cross-sectional area of each ply with the increase in the distance from the surface where the electrodes are located. σ_{mn}^k $(m, n = \xi, \eta)$ is the electric conductance of ξ and η direction of the kth ply.

For applied thick CFRP laminates, the main issue is how to decide the contribution function $F(\alpha)$. As the electric current usually flows in the direction that has high electric conductance, let us consider the case where the electric current flows in the fiber direction of the surface ply. To obtain the contribution function with simple calculations, it is assumed that the distribution of the difference in the voltages of the laminated CFRP used in practice is independent of the stacking sequence when the spacing between the electrodes is the same value. On the basis of this assumption, we can use the distribution of the electric current density for the unidirectional thick CFRP. The difference in the voltages can be easily calculated from the electric current density obtained using the analytical method of the previous study.[3] After calculating the difference in the voltages, normalization by the division of the value at $z = 0$ determines the contribution function F.

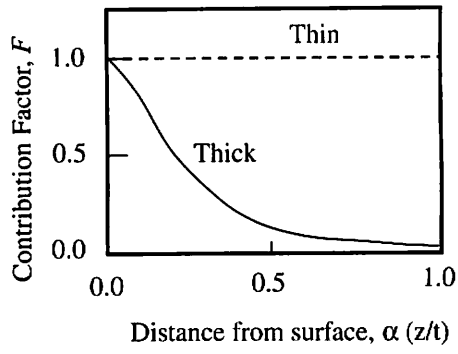

Fig. 3. Definition of the contribution function.

There are two distributions of the difference in the voltages: the x-axis and y-axis. These two distributions can be used to obtain F_x and F_y. However, there is no interaction term in unidirectional CFRP, and this makes it impossible to obtain the interaction term $C_{\xi\eta}$. Of course, we may obtain the approximated distribution of F_{xy} using the mean values of F_x and F_y.

In the thick laminated CFRP plate used in practice, positive and negative angle plies are placed close to each other to prevent bending and twisting coupling. We can approximately consider the two plies as a uniform single ply of coupled angle plies (positive angle and negative angle). The coupling of the angle plies deletes the interaction term $C_{\xi\eta}$. This means we do not need to obtain F_{xy}. The most typically used angle ply is $+45°$ and $-45°$ ply for actual CFRP laminates. Thus, we replace these two plies with a single $\pm 45°$ ply of twice the thickness.

We now need to make sure the condition for the approximation of the thick CFRP (the infinite-body approximation) is satisfied as mentioned in the previous study.[3] For the approximation, the infinite-body condition must be satisfied as follows.

$$\frac{t}{a\lambda} \geq 6.3, \qquad (12)$$

$$\lambda = \sqrt{\sigma_z/\sigma_x}, \qquad (13)$$

where $2a$ is spacing between the electrodes and t is thickness of the CFRP laminate.

When the condition of the infinite-body approximation is not satisfied, the analysis is not appropriate. This means the

laminate is not a thick CFRP plate. When the laminate is neither thick nor thin enough, the 2D-FEM analysis of unidirectional CFRP can be used to obtain the contribution function F. FEM analysis of a 2D cross-section that includes the line segment of the two electrodes gives an appropriate distribution of difference in the voltages. Since the distribution becomes a bilaterally-symmetric distribution at $x = 0$ (the middle of the two electrodes), the distribution at $x = \pm a/2$ is a good reference for the distribution function.

The contribution function is affected by the difference in the transverse direction between the conductance in the thickness and in the fiber directions. The conductance ratio is important. The configuration function can be calculated easily using the potential flow of a perfect fluid coupled with a source and sink.[3)]

The spacing between the electrodes (a) cannot be obtained for the case of the leakage electric current from a lightning strike. Since the exact value is not so important, the spacing between the metallic parts or the length of plate can be used for the practical analysis of a lightning strike. Estimating the accuracy is planned in future work.

3. Comparison between FEM and Analysis

3.1. Difference in the voltages

We now consider the case of a square plate 40-mm-long and 4-mm-thick as shown in Fig. 4. The origin of the rectangular coordinates is set to the middle point of the surface of the square plate: the thickness direction (z) has its origin at the surface $z = 0$. We consider the case for the combination of a source at $(-4, 0, 0)$ and a sink at $(4, 0, 0)$ located on the x axis with spacing of 8 mm. Here we have the electric conductance in the fiber direction σ_x of 1 A/mm^2, the electric conductance in the fiber direction σ_y of 0.1 A/mm^2, and the electric conductance in the thickness direction σ_z of 0.01 A/mm^2. This combination of electric conductance corresponds to strongly orthotropic CFRP.[1)] The applied electric current is 1 A. For the FEM analysis, the commercially available ANSYS is used. The total number of elements for the 3D-FEM analysis is 286,720, and the total number of nodes is 1,440,820. The minimum length of an element is 0.1 mm.

The stacking sequence of the CFRP plate is $[0/45/-45/90/0/0/90/-45/45/0]_T$. The total number of plies is 10. The thickness of each ply is 0.4 mm. For the CFRP plate, 0° is the direction of the x-axis, and 90° is the direction of the y-axis. The positive z-direction is the thickness direction from the surface. The positive rotation angle of the ply is a counterclockwise rotation viewed from the surface.

Using the same specimen configuration shown in Fig. 4 with unidirectional CFRP: A current of 1 A is applied at point A and the voltage is set to 0 V.[3)] Comparison of the difference in the voltages between the laminated CFRP obtained from the 3D-FEM and the unidirectional CFRP obtained from the infinite-body approximation is performed at the B-B′ and D-D′ line segments. The difference in the

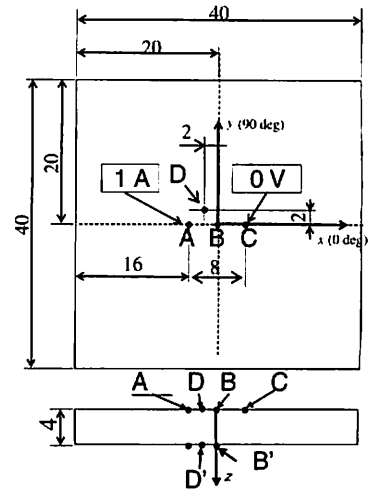

Fig. 4. Specimen configuration and the coordinates.

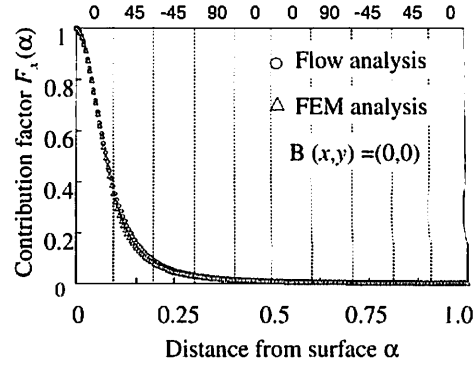

Fig. 5. F_x distribution of the B-B′ line.

voltages in the x-direction is compared at the B-B′ line segment and the difference in the voltages at the D-D′ line segment of the x-axis/y-axis is compared. For calculating the contribution function, the difference in the voltages is normalized using the value at $x = 0$ to obtain a value of one at $z = 0$. As a typical example, the contribution function for the x-axis F_x at point B is shown in Fig. 5. Figure 6 shows the results of the contribution function F_x for the x-axis at point D. Figure 7 shows the results of contribution function F_y of y-axis at point D. In these figures, the ordinate shows the values of the contribution function, which is obtained by normalizing the difference in the voltages. The abscissa is α, and the depth from the surface normalized by the thickness. The broken perpendicular lines in the figure indicate the plies.

From these figures, the contribution functions can be approximated from the differences in the voltages obtained with the infinite-body approximation of unidirectional CFRP.

To investigate the configuration of the contribution function, the value of the contribution functions at six points ($x = 0, -1, -2, -3, -4, -5$ mm) and $y = 1$ mm are compared in Fig. 8. The ordinate is the contribution function F_x and the abscissa is the normalized depth α. The electrodes are located at $x = -4$ mm and $x = 4$ mm. The four contribution function values $x = 0, -1, -2$ and -3 mm that

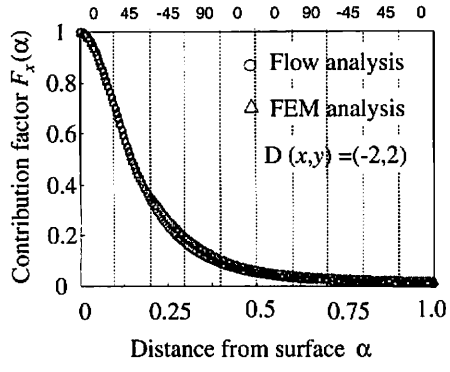

Fig. 6. F_x distribution of the D-D' line.

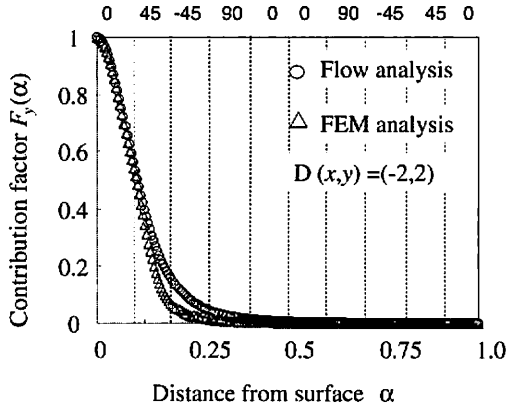

Fig. 7. F_y distribution of the D-D' line.

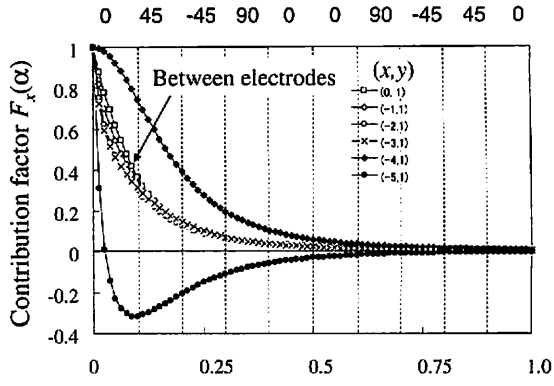

Fig. 8. Variation of F_x at constant $y = 1$ mm.

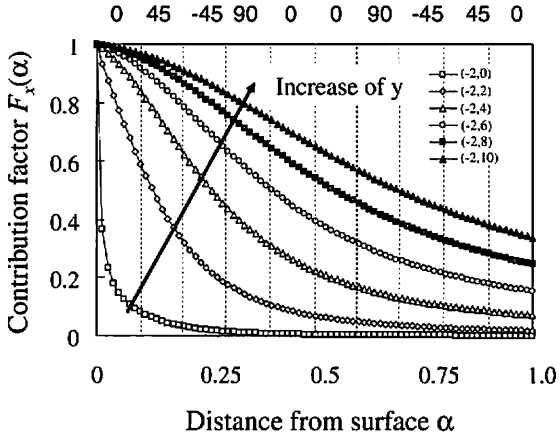

Fig. 9. Variation of F_x at constant $x = -2$ mm.

are located between the electrodes have a similar shape. The point $x = -5$ mm is located behind the electrode where the electric current is applied. At this point, the electric current flows in a backward direction near the surface and in a forward direction in the deep area. The absolute amount of electric current, however, is very small compared with the area between the electrodes.

Similarly, the variation of the contribution function F_x at the constant $x = -2$ mm is shown in Fig. 8. Six locations of $y = 2$, 4, 6, 8 and 10 mm are selected as parameters. As shown in Fig. 9, when moving from the line segment between the electrodes (an increase in y), the contribution function becomes flat. The contribution function indicates that near the electrode line segment (the data for $y = 2$ mm), 90% of the electric current flows in the surface of the 0° ply, 7% of the electric current flows in the second 45° ply and 1% of the electric current flows in the third −45° ply.

3.2. Comparison of results

The calculation results using the thin and thick lamination theory are compared with the results obtained from the 3D-FEM results.

Using the thin lamination theory, the electric conductance values for 2D-FEM analysis are obtained: $\sigma_x = 0.64$ S/mm and $\sigma_y = 0.46$ S/mm. The thin lamination theory provides uniform electric conductance over the entire laminate.

The thick lamination theory requires the analysis of infinite-body approximation to obtain the electric current density. From the electric current density distribution at the center point of each 2D-FEM element, the contribution function of each element is calculated, and the electric conductance of each element is calculated using the contribution function. The calculated electric conductance differs between the elements. In this study, the square specimen is modeled for 2D-FEM with 1,600 elements (40 × 40). Since thick lamination theory deals with ±45° ply as a single ply of twice the thickness, we do not need to consider the angle plies. This means that a quarter of the specimens are adequate for the calculations because of symmetry. Thus, the total number of elements for 2D-FEM is 400 (20 × 20). When all the elements require different electric conductance, it is very time consuming. As shown in Figs. 8 and 9, the contribution function is almost the same when the distance from the line segment between the electrodes is the same. Moreover, the electric current at the rear of the electrodes is very small.

As shown in Fig. 9, the contribution function near $y = 0$ is very steep and becomes smooth with the increase in y. In this study, therefore, the area is divided into three subareas: area #1 from $y = 0$ mm to $y = 4$ mm, area #2 from $y = 4$ mm to $y = 10$ mm and area #3 from $y = 10$ mm to the boundary. In each area, uniform conductance is adopted to prevent cumbersome data input jobs. The center point of the area is adopted to calculate the conductance. Thus, only

Table 1. Electric conductance in three areas.

Region	σ_x [S/mm]	σ_y [S/mm]
(1) 0–4 [mm]	0.12	0.019
(2) 4–10 [mm]	0.30	0.15
(3) 10–20 [mm]	0.48	0.30

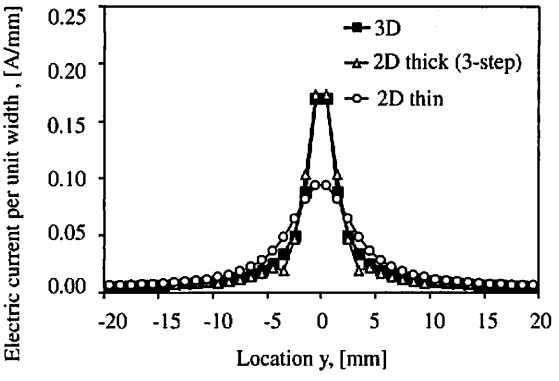

Fig. 10. Comparison between 2D-FEM and 3D-FEM.

three types of conductance are used in the calculation in this study. The calculated conductance is shown in Table 1.

Using the calculated conductance of the three areas, 2D-FEM is performed with equally square elements of 1 mm length. The total number of elements is 1,600. To compare the results with 3D-FEM, the electric current density of 3D-FEM results is integrated in the thickness direction with a width of 1 mm at $x = 0$ mm. Figure 10 shows the results of the comparison.

The abscissa is the location of the y-direction, and the ordinate is the electric current density at $x = 0$ of unit width. Open circle symbols indicate the 2D-FEM results using the thin lamination theory and the triangular symbols indicate the 2D-FEM results of the thick lamination theory. The solid square symbols indicate the 3D-FEM results. Comparing the electric current near $y = 0$, the thin lamination theory has 80% error. On the other hand, the thick lamination theory has only 4% error. In 3D-FEM analysis, mesh division is fully refined until no difference in the results is obtained with the refinement of mesh division. The total number of elements for 2D-FEM analysis in the thick lamination theory is only 1,600/286,720 = 0.56% of the 3D-FEM calculation of the electric current density. This shows that the thick lamination theory is quite effective for electric current calculations of the typical applied thick CFRP laminates.

In the previous paper,[3] Eq. (12) was proposed as the thick CFRP criterion rule. In this study, $t = 4$ mm, $a = 4$ mm, $\lambda = 0.1$, and the condition is satisfied. When the spacing between the electrodes exceeds $a = 6.3$ mm, the infinite-body approximation is not applied.

As an example, let us consider the case of $2a = 24$ mm. The source is located at $(-12, 0, 0)$ and the sink at $(12, 0, 0)$. In this situation, Eq. (12) is not satisfied. Thus, the infinite-body approximation is not appropriate for this model. To obtain the contribution function, 2D-FEM analysis is performed in the x–z plane of $y = 0$. The total number

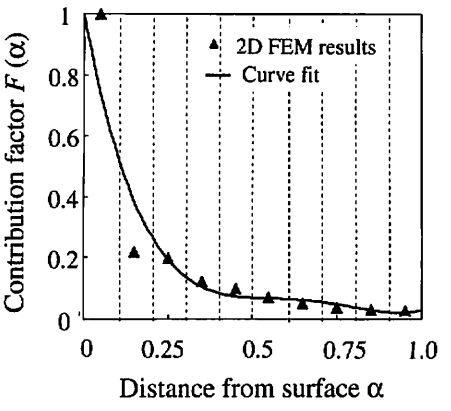

Fig. 11. F_x obtained from the cross-section FEM.

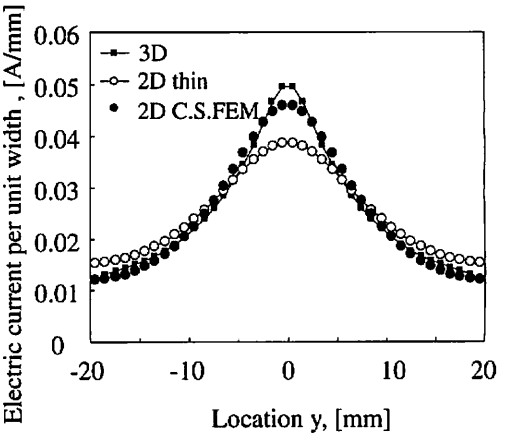

Fig. 12. Comparison of FEM results when the thick condition is not satisfied.

of elements for the analysis is 1,000. As a sampling point, the electric current density distribution at $x = -a/2$ is obtained and the contribution function is calculated from the results. Figure 11 shows the contribution function used for the analysis. For the calculations of electric conductance, the solid curve in Fig. 11 is obtained using the least-square-error method.

The results obtained are $\sigma_x = 0.117$ S/mm and $\sigma_y = 0.053$ S/mm. Using the value obtained, 2D-FEM analysis is performed and the results are compared with the 3D-FEM results. Figure 12 shows the results of the comparison. The open symbols indicate the results of the thin lamination theory, and the solid circle symbols indicate the results of 2D-FEM analysis in a new lamination theory with the cross-section FEM analysis. The solid square symbols indicate the 3D-FEM analysis. Near the line segment of $y = 0$, the thin lamination theory has a 28% error, but the 2D-FEM results of the new lamination theory with the cross-section FEM have only an 8% error.

4. Conclusions

In this study, a new lamination theory to obtain electric conductance was proposed for strongly orthotropic CFRP laminates. Using the potential flow analysis for thick CFRP laminates, the contribution function was calculated and the

electric conductance obtained. The results were compared with 3D-FEM analysis. In summary,

(1) A lamination theory for thin laminates was illustrated.
(2) A new lamination theory for applied thick CFRP laminates using a contribution function was proposed.
(3) Comparison of the results with 3D-FEM analysis showed that the new theory gives excellent approximations for 2D-FEM analysis.
(4) Even for typical laminates, in practice, this does not satisfy the condition for thick CFRP laminates, and the contribution function can be obtained using the cross-section 2D-FEM analysis.

References

1) Todoroki, A., Tanaka, M. and Shimamura, Y.: Measurement of Orthotropic Electric Conductance of CFRP Laminates and Analysis of the Effect on Delamination Monitoring with Electric Resistance Change Method, *Compos. Sci. Tech.*, **62** (2002), pp. 619–628.
2) Hirano, Y., Katsumata, S., Iwahori, Y. and Todoroki, A.: Artificial Lightning Testing on Graphite/epoxy Composite Laminate, *Composites A*, **41** (2010), pp. 1461–1470.
3) Todoroki, A.: Electric Current Analysis of CFRP using Perfect Fluid Potential Flow, *Trans. Jpn. Soc. Aeronaut. Space Sci.*, **55** (2012), pp. 183–190.
4) Xiao, J., Li, Y. and Fan, W. X.: A Laminate Theory of Piezoresistance for Composite Laminates, *Compos. Sci. Tech.*, **59** (1999), pp. 1369–1373.
5) Özisik, M. N.: *Heat Conduction*, 2nd ed., John Wiley & Sons Inc., New York, 1993.